



# Synthesis and performance of new quinoxaline-based dyes for dye sensitized solar cell



Chang Young Jung, Cheol Jun Song, Wang Yao, Jong Min Park, In Ho Hyun, Dong Hoon Seong, Jae Yun Jaung\*

Department of Organic and Nano Engineering, Hanyang University, 222 Wangsimni-ro, Seongdong-gu, Seoul 133-791, South Korea

## ARTICLE INFO

*Article history:*  
Received 24 March 2015  
Received in revised form  
13 May 2015  
Accepted 17 May 2015  
Available online

*Keywords:*  
Quinoxaline  
Triphenylamine  
Phenothiazine  
Dye-sensitized solar cells  
Sensitizers  
IPCE

## ABSTRACT

New quinoxaline-based dyes were synthesized and applied as a sensitizer for dye-sensitized solar cell. A quinoxaline moiety was used as an electron withdrawing group and triphenylamine and phenothiazine derivatives were introduced as electron donating groups. The dyes synthesized with the phenothiazine moiety showed greater conversion efficiency than dyes with the triphenylamine moiety leading to the best overall power conversion efficiency of 4.36%.

© 2015 Elsevier Ltd. All rights reserved.

## 1. Introduction

With increasing interest in alternative energy, researchers have focused on solar energy due to its sustainability and ease of access. Dye-sensitized solar cells (DSSC) convert light to electric energy [1]. DSSCs have attracted research because of their low cost and high power-conversion efficiency [2]. Dye molecules play a key role as sensitizers and have been studied to improve the efficiency of the solar energy to electricity conversion in DSSC [3]. Grätzel reached an efficiency of over 11% using N719 dye, a Ru-metal complex [4]; however, this dye is inefficient for large scale applications because the ruthenium atom is rare and expensive. For those reasons, metal-free dyes have gained interest due to easily-tunable absorption regions, high molecular extinction coefficients and lower cost when compared to metal complexes. Carbazole [5], coumarin [6], indoline [7,8], porphyrin [9,10], perylene [11,12], phthalocyanine [13,14], phenothiazine [15–18], squaraine [19] have been introduced in the literature as sensitizers for improving efficiency. Recently, the Grätzel group achieved an efficiency of 13% using porphyrin dye [20].

Generally, metal-free dyes for DSSCs feature a push-pull structure, in which the electron transfer occurs efficiently. Once the electrons in the dye are excited due to the absorption of light, an electron donor pushes and an electron acceptor pulls the electrons from the donor. The electrons transported to the acceptor can be injected into the conduction band of a semiconductor through anchoring groups linked to the acceptor.

Over the last several decades, various functional groups and their derivatives have been introduced as electron donors or acceptors. Among these, triphenylamine derivatives are excellent electron donors due to their electron-donating property and non-planar molecular configuration, which prevents aggregation [21,22].

Phenothiazine derivatives have shown better light conversion efficiency than similarly-shaped triphenylamine groups because a phenothiazine moiety with electron-rich heteroatoms, nitrogen and sulfur, has a strong electron donating ability. In addition, a non-planar structure like butterfly suppresses aggregation via intermolecular interaction [23].

Quinoxaline moieties have recently been investigated as electron acceptors in DSSCs, utilizing their strong electron-withdrawing property that stems from a high electron affinity derived from two symmetric unsaturated nitrogen atoms in the heterocycle [24]. Dong Wook Chang et al. [25] modified horizontally- or vertically-structured quinoxaline derivatives, and Takahiro

\* Corresponding author. Tel.: +82 2 2220 0492; fax: +82 2 2220 4092.  
E-mail address: [jjy1004@hanyang.ac.kr](mailto:jjy1004@hanyang.ac.kr) (J.Y. Jaung).

Kono et al. [26] and Jie Shi et al. [27] studied quinoxaline-based DSSCs using the triphenylamine group as the electron donor, though neither study has introduced more powerful electron donors such as triphenylamine derivatives with alkoxy moieties. To the best of our knowledge, there has not yet been any attempt to utilize the phenothiazine and quinoxaline groups as electron donors and acceptors, respectively, for DSSCs.

In this study, triphenylamine and phenothiazine derivatives with an alkoxy group were introduced to 2, 3-positions of quinoxaline as an electron donor for the Y-shape, and a carboxylic group was introduced to the 6-position as an anchoring group. Introduction of the alkoxy groups on the electron donor was expected to improve the electron donating ability. The synthesized structures, **NQX1-4**, exhibited photovoltaic properties.

## 2. Experimental

### 2.1. Materials

All reagents and solvents were purchased commercially and used without further purification. (isopentyloxy)benzene, 4-(bis(4-methoxyphenyl)amino)benzaldehyde (**3a**), 10-(4-methoxyphenyl)-10H-phenothiazine-3-carbaldehyde (**5a**) and 4-acetamidobenzoic acid (**6**) were prepared following methods reported in literature [23,28–30].

### 2.2. Characterization

$^1\text{H}$  and  $^{13}\text{C}$  NMR spectra were recorded on a VARIAN UnityInova 300 MHz FT-NMR spectrometer. MALDI-TOF MS analysis was conducted on a Waters Limited MALDI-TOF spectrometer using a dithranol matrix. The UV–vis absorption spectra were measured on a Jasco V-670 spectrophotometer. Cyclic voltammetry (CV) was performed on a Bio-Logic (SP-200) with a three-electrode cell in DMF containing 0.1 M tetrabutylammonium hexafluorophosphate at a scan rate of 100  $\text{mVs}^{-1}$ . A carbon electrode, Ag/AgCl electrode, and a platinum wire were used as working, reference, and counter electrodes, respectively.

### 2.3. DSSC fabrication

A 0.1M titanium (IV) bis(ethyl acetoacetate)diisopropoxide solution in butanol was coated on the FTO glass plate (Pilkington-TEC8) by a spin coater (at 1000 rpm for 10s and then, at 2000 rpm for 40s) and the substrate was heated to 450 °C for 30 min in a furnace to form a 20-nm thickness. A 20-nm  $\text{TiO}_2$  paste (PST-18 NR, CCIC) was coated by a doctor blading method and annealed at 450 °C for 30 min (~11  $\mu\text{m}$ ). The scattering layer was developed by a doctor blading method using a 400-nm  $\text{TiO}_2$  particle (PST-400C, CCIC) and treated under 450 °C for 30 min (~4  $\mu\text{m}$ ) to improve light absorption. The treated substrate was further exposed to an aqueous 50 mM  $\text{TiCl}_4$  solution at 70 °C for 20 min and sintered at 450 °C for 30 min. After sintering, the substrate was immersed in a  $5 \times 10^{-4}$  M dye solution of chloroform for 2 h at room temperature for dye adsorption (in the case of N719 dye, the substrate was immersed for 24 h), rinsed with chloroform and dried. To prepare the counter electrode, a 0.01M  $\text{H}_2\text{PtCl}_6$  solution in isopropyl alcohol was coated on the cleaned FTO plate using a spin coater (at 1000 rpm for 10s and at 2000 rpm for 40s, subsequently) and heated at 450 °C for 30 min. The Pt-coated electrode was then drilled to make two holes, washed with ionized water and dried. The prepared electrodes were assembled into a sandwich-type structure using surlyn film (25  $\mu\text{m}$ ) with a hot press at 90 °C. After assembly, an electrolyte solution (0.6 M DMPII, 0.1M LiI, 0.1M  $\text{I}_2$ , 0.5M TBP in acetonitrile) was injected into the cell through the

holes and the holes were sealed with a cover glass using the additional surlyn film. The active area of the dye-coated  $\text{TiO}_2$  film was 0.25  $\text{cm}^2$ .

### 2.4. Measurements

The photocurrent density-voltage (J-V) curves were collected using a Keithley Model 2400 source meter and a solar simulator with a 300W Xenon arc-lamp Newport under AM 1.5 illumination (100  $\text{mWcm}^{-2}$ ). A photomask on the residual area of the dye fabricated cell was used to reduce scattered light (the active area of the DSSC was 0.25  $\text{cm}^2$ ). The incident photon-current conversion efficiency (IPCE) was recorded in the wavelength range of 300–800 nm using a model QEX7 solar cell spectral response measurement system (PV Measurements, Inc).

### 2.5. Synthesis

#### 2.5.1. 1-iodo-4-(isopentyloxy)benzene (**1b**)

Sulfuric acid (24.2 ml) was carefully added to methanol (400 ml) in a 3-neck flask under stirring and then cooled to 0 °C. Potassium iodide (50.7 g, 1.82 mol) and (isopentyloxy)benzene (49.2 g, 0.3 mol) was slowly added sequentially to the solution. After warming to room temperature, 30% hydrogen peroxide (63.6 ml) was slowly added drop wise and then stirred at 60 °C for 14 h. The resulting mixture was cooled to room temperature, poured into water and extracted with chloroform. The organic phase was washed with a sodium metabisulfate aqueous solution, dried over anhydrous sodium sulfate, and concentrated to produce a yellow oil (87 g, 0.3 mol).  $^1\text{H}$  NMR (300 MHz,  $(\text{CD}_3)_2\text{SO}$ ):  $\delta$  (ppm) = 7.58–7.55 (d,  $J$  = 9.0 Hz, 2H, ArH), 6.79–6.76 (d,  $J$  = 9.0 Hz, 2H, ArH), 3.97–3.93 (t,  $J$  = 6.6 Hz, 2H,  $-\text{CH}_2-$ ), 1.80–1.70 (m,  $J$  = 6.6 Hz, 1H,  $-\text{CH}-$ ), 1.61–1.55 (q,  $J$  = 6.6 Hz, 2H,  $-\text{CH}_2-$ ), 0.92–0.89 (d, 6H,  $-\text{CH}_3$ ).  $^{13}\text{C}$  NMR (150 MHz,  $(\text{CD}_3)_2\text{SO}$ ):  $\delta$  (ppm) = 158.5, 137.9, 117.2, 82.8, 66.0, 37.3, 24.5, 22.4.

#### 2.5.2. 4-(isopentyloxy)-N-(4-(isopentyloxy)phenyl)-N-phenylaniline (**2b**)

Copper powder (26.8 g, 0.42 mol) and copper iodide (0.187 g, 0.98 mmol) were added to a solution of **1b** (87 g, 0.3 mol) and aniline (13.1 g, 0.14 mol) in *o*-dichlorobenzene (100 ml), and potassium carbonate (77.6 g, 0.56 mol) under a  $\text{N}_2$  condition. The resulting mixture was vigorously refluxed for 24 h, cooled to room temperature and filtered with benzene. The filtrate was concentrated and purified by column chromatography on silica gel using dichloromethane/hexane (1:2) as an eluent. The yield of the yellow viscous liquid was 35 g (60%).  $^1\text{H}$  NMR (300 MHz,  $\text{CDCl}_3$ ):  $\delta$  (ppm) = 7.22–7.17 (t, 2H, ArH), 7.09–7.06 (d,  $J$  = 9.0 Hz, 4H, ArH), 6.99–6.97 (d,  $J$  = 7.5 Hz, 4H, ArH), 6.94–6.89 (t,  $J$  = 7.5 Hz, 1H, ArH), 6.87–6.84 (d,  $J$  = 9.0 Hz, 2H, ArH), 4.01–3.97 (t,  $J$  = 6.6 Hz, 4H,  $-\text{CH}_2-$ ), 1.93–1.84 (m,  $J$  = 6.6 Hz, 2H,  $-\text{CH}-$ ), 1.75–1.68 (q,  $J$  = 6.6 Hz, 4H,  $-\text{CH}_2-$ ), 1.02–1.00 (d, 12H,  $-\text{CH}_3$ ).  $^{13}\text{C}$  NMR (150 MHz,  $\text{CDCl}_3$ ):  $\delta$  (ppm) = 155.2, 148.8, 140.9, 128.8, 126.3, 120.7, 115.3, 115.1, 66.5, 38.1, 25.0, 22.6.

#### 2.5.3. 4-(bis(4-(isopentyloxy)phenyl)amino)benzaldehyde (**3b**)

The solution of **2b** (30 g, 0.072 mol) in DMF (320 ml) was stirred at 0 °C. Phosphorus oxychloride (17.7 g, 0.115 mol) was added drop wise, and stirred at room temperature for an additional 30 min. The resulting mixture was heated to 80 °C, stirred for 12 h, cooled to room temperature, and poured into water. After stirring for 30 min, the emulsion was extracted with ether. The organic solvent was washed with brine, dried over anhydrous sodium sulfate and concentrated. The residue was purified by column chromatography on silica gel using chloroform as an eluent to produce a yellow

viscous liquid product (18.9 g, 59%).  $^1\text{H}$  NMR (300 MHz,  $\text{CDCl}_3$ ):  $\delta$  (ppm) = 9.75 (s, 1H, -CHO), 7.64–7.61 (d,  $J$  = 8.7 Hz, 2H, ArH), 7.13–7.10 (d,  $J$  = 9.0 Hz, 4H, ArH), 6.90–6.83 (m, 6H, ArH), 4.00–3.96 (t,  $J$  = 6.6 Hz, 4H,  $-\text{CH}_2-$ ), 1.90–1.81 (m,  $J$  = 6.6 Hz, 2H,  $-\text{CH}-$ ), 1.72–1.65 (q,  $J$  = 6.6 Hz, 4H,  $-\text{CH}_2-$ ), 0.99–0.96 (d, 12H,  $\text{CH}_3$ ).  $^{13}\text{C}$  NMR (150 MHz,  $\text{CDCl}_3$ ):  $\delta$  (ppm) = 190.2, 156.8, 154.0, 138.5, 131.3, 128.0, 127.6, 116.6, 115.5, 66.5, 37.9, 24.9, 22.5.

#### 2.5.4. 10-(4-(isopentyloxy)phenyl)-10H-phenothiazine (**4b**)

**1b** (87 g, 0.3 mol), phenothiazine (40.8 g, 0.2 mol), copper powder (25.4 g, 0.4 mol), potassium carbonate (111 g, 0.8 mol) and 18-crown-6 (5.2 g, 0.02 mol) were suspended in *o*-dichlorobenzene (230 ml) under a  $\text{N}_2$  condition. The suspension was refluxed for 24 h and then cooled to room temperature and filtered with chloroform. The filtrate was evaporated in vacuo, and then purified by recrystallization with methanol to produce an ivory solid (59 g, 80%). m.p. 90 °C.  $^1\text{H}$  NMR (300 MHz,  $(\text{CD}_3)_2\text{SO}$ ):  $\delta$  (ppm) = 7.33–7.30 (d,  $J$  = 9.0 Hz, 2H, ArH), 7.21–7.18 (d,  $J$  = 9.0 Hz, 2H, ArH), 7.05–7.03 (d,  $J$  = 7.5 Hz, 2H, ArH), 6.94–6.80 (m, 4H, ArH), 6.16–6.13 (d,  $J$  = 8.1 Hz, 2H, ArH), 4.10–4.06 (t,  $J$  = 6.6 Hz, 2H,  $-\text{CH}_2-$ ), 1.85–1.78 (m,  $J$  = 6.6 Hz, 1H,  $-\text{CH}-$ ), 1.70–1.63 (q,  $J$  = 6.6 Hz, 2H,  $-\text{CH}_2-$ ), 0.97–0.95 (d, 6H,  $-\text{CH}_3$ ).  $^{13}\text{C}$  NMR (150 MHz,  $(\text{CD}_3)_2\text{SO}$ ):  $\delta$  (ppm) = 158.4, 144.0, 132.2, 131.9, 127.2, 126.5, 122.4, 118.7, 116.5, 115.5, 66.2, 37.4, 24.6, 22.4.

#### 2.5.5. 10-(4-(isopentyloxy)phenyl)-10H-phenothiazine-3-carbaldehyde (**5b**)

The solution of **4b** (30 g, 83.0 mmol) and DMF (67.8 ml, 829.9 mmol) in 1,1,2-trichloroethane (200 ml) was stirred at 0 °C. Phosphorus oxychloride (31 ml, 332.0 mmol) was slowly added to the solution, stirred at 0 °C for 30 min, and heated to 95 °C. After stirring for an additional 4 h, the mixture was cooled to room temperature, poured into ice water and stirred for 30 min. The emulsion was extracted with chloroform. The organic phase was dried over anhydrous sodium sulfate, concentrated with an in vacuo rotary evaporator and purified by column chromatography on silica gel using benzene as an eluent to produce a yellow solid product (25.5 g, 79%). m.p. 105 °C.  $^1\text{H}$  NMR (300 MHz,  $\text{CDCl}_3$ ):  $\delta$  (ppm) = 9.68 (s, 1H, -CHO), 7.44 (s, 1H, ArH), 7.29–7.24 (m, 3H, ArH), 7.13–7.10 (d,  $J$  = 8.7 Hz, 2H, ArH), 6.96–6.93 (m, 1H, ArH), 6.84–6.81 (m, 2H, ArH), 6.21–6.18 (d,  $J$  = 8.7 Hz, 1H, ArH), 6.18–6.14 (m, 1H, ArH), 4.09–4.05 (t,  $J$  = 6.6 Hz, 2H,  $-\text{CH}_2-$ ), 1.94–1.85 (m,  $J$  = 6.6 Hz, 1H,  $-\text{CH}-$ ), 1.78–1.71 (q,  $J$  = 6.6 Hz, 2H,  $-\text{CH}_2-$ ), 1.02–1.00 (d, 6H,  $-\text{CH}_3$ ).  $^{13}\text{C}$  NMR (150 MHz,  $\text{CDCl}_3$ ):  $\delta$  (ppm) = 189.7, 159.2, 149.5, 142.8, 132.0, 131.6, 130.8, 129.9, 127.4, 127.0, 126.5, 123.5, 119.9, 118.9, 116.6, 116.4, 114.9, 66.7, 37.9, 25.0, 22.6.

#### 2.5.6. 2,3-dimethylquinoxaline-6-carboxylic acid (**7**)

**6** (5 g, 27.5 mmol) and tin chloride dehydrate (31.0 g, 137.3 mmol) were suspended in ethanol (30 ml) under  $\text{N}_2$  conditions. The suspension was refluxed for 5 h, and then cooled to room temperature. 2,3-butandione (2.37 g, 27.5 mmol) was added to the suspension and the suspension was refluxed for an additional hour. The resulting mixture was cooled to room temperature, alkalinized to pH 11 by adding a 2M NaOH aqueous solution. The alkalinized suspension was filtered using celite, and the filtrate was evaporated to remove the organic solvent. The residue was acidified to pH 2 with a 2M HCl aqueous solution, and then the precipitate was filtered, and purified by recrystallization with methanol. The product was obtained as a gray solid to produce 5.1 g (92%). m.p. 230 °C.  $^1\text{H}$  NMR (300 MHz,  $(\text{CD}_3)_2\text{SO}$ ):  $\delta$  (ppm) = 13.25 (br, 1H, -COOH), 8.43 (s, 1H, ArH), 8.18–8.15 (d,  $J$  = 8.4 Hz, 1H, ArH), 8.00–7.97 (d,  $J$  = 8.4 Hz, 1H, ArH), 2.71 (s, 6H,  $-\text{CH}_3$ ).  $^{13}\text{C}$  NMR (150 MHz,  $(\text{CD}_3)_2\text{SO}$ ):  $\delta$  (ppm) = 166.8, 156.1, 155.2, 142.4, 139.5, 130.6, 130.0, 128.4, 128.0, 23.0, 22.8.

#### 2.5.7. 2,3-bis((E)-4-(bis(4-methoxyphenyl)amino)styryl)quinoxaline-6-carboxylic acid (**NQX1**)

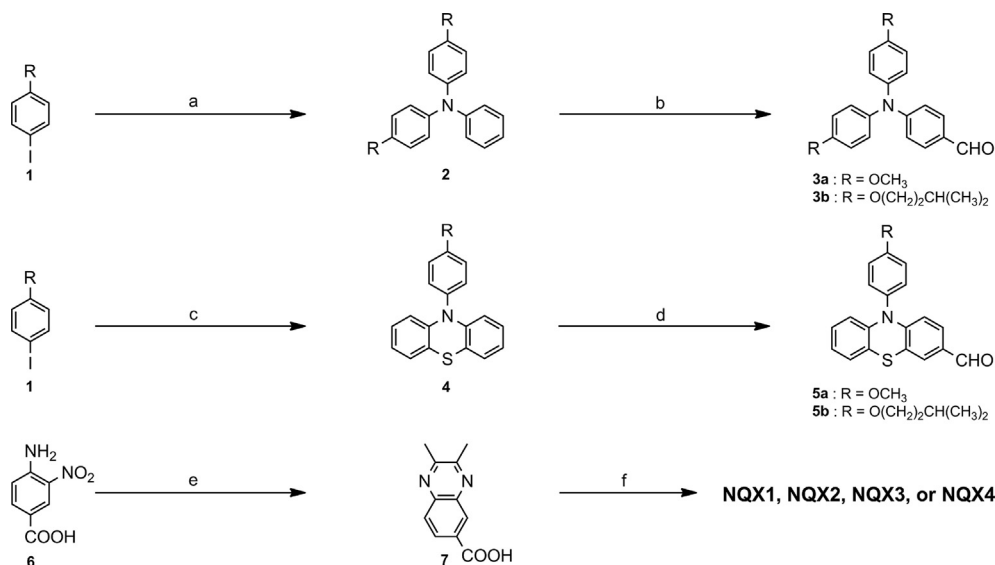
A mixture of **7** (0.26g, 1.0 mmol), **3a** (0.9g, 2.1 mmol) and a small portion of piperidine in anhydrous toluene (10 ml) was refluxed under a  $\text{N}_2$  atmosphere. The reaction was confirmed using thin layer chromatography. After cooling to room temperature, the remaining liquid was concentrated and purified by column chromatography on silica gel using chloroform/methanol (20:1) as an eluent to produce a red-brown solid product (0.9 g, 84%). m.p. 165 °C.  $^1\text{H}$  NMR (300 MHz,  $(\text{CD}_3)_2\text{SO}$ ):  $\delta$  (ppm) = 13.29 (br, 1H, -COOH), 8.44 (s, 1H, ArH), 8.11–8.07 (d,  $J$  = 8.7 Hz, 1H, ArH), 7.97–7.88 (m, 3H, ArH,  $-\text{CH}-$ ), 7.72–7.66 (m, 6H, ArH,  $-\text{CH}-$ ), 7.10–7.07 (d,  $J$  = 9.0 Hz, 8H, ArH), 6.95–6.92 (d,  $J$  = 9.0 Hz, 8H, ArH), 6.74–6.70 (m, 4H, ArH), 3.75 (s, 12H,  $-\text{CH}_3$ ).  $^{13}\text{C}$  NMR (150 MHz,  $(\text{CD}_3)_2\text{SO}$ ):  $\delta$  (ppm) = 166.7, 156.3, 150.5, 150.0, 149.5, 149.4, 142.7, 139.9, 139.2, 138.3, 137.8, 130.7, 129.4, 129.3, 128.3, 127.4, 127.2, 118.4, 117.8, 117.7, 115.0, 55.4. MS (MALDI-TOF)  $m/z$  832.32. Calcd: 832.94. Anal. Calcd for  $\text{C}_{53}\text{H}_{44}\text{N}_4\text{O}_6$ : C, 76.42; H, 5.32, N, 6.73. Found: C, 76.07; H, 5.68, N, 6.51.

#### 2.5.8. 2,3-bis((E)-4-(bis(4-(isopentyloxy)phenyl)amino)styryl)quinoxaline-6-carboxylic acid (**NQX2**)

**NQX2** was synthesized with a method similar to **NQX1**. A mixture of **7** (0.44 g, 2.18 mmol), **3b** (2.1 g, 4.71 mmol) and a small portion of piperidine in anhydrous toluene (20 ml) was refluxed under a  $\text{N}_2$  condition. The reaction was confirmed using thin layer chromatography. After cooling to room temperature, the remaining liquid was concentrated and purified by column chromatography on silica gel using chloroform/methanol (20:1) as an eluent to produce a red-brown solid product (1.1 g, 48%). m.p. 135 °C.  $^1\text{H}$  NMR (300 MHz,  $(\text{CD}_3)_2\text{SO}$ ):  $\delta$  (ppm) = 13.30 (br, 1H, -COOH), 8.45 (s, 1H, ArH), 8.12–8.08 (d,  $J$  = 8.7 Hz, 1H, ArH), 7.99–7.89 (m, 3H, ArH,  $-\text{CH}-$ ), 7.74–7.66 (m, 6H, ArH,  $-\text{CH}-$ ), 7.07–7.04 (d,  $J$  = 8.4 Hz, 8H, ArH), 6.93–6.90 (d,  $J$  = 8.4 Hz, 8H, ArH), 6.73–6.67 (m, 4H, ArH), 3.98–3.93 (t,  $J$  = 6.6 Hz, 8H,  $-\text{CH}_2-$ ), 1.82–1.73 (m,  $J$  = 6.6 Hz, 4H,  $-\text{CH}-$ ), 1.63–1.56 (q,  $J$  = 6.6 Hz, 8H,  $-\text{CH}_2-$ ), 0.93–0.91 (d, 24H,  $-\text{CH}_3$ ).  $^{13}\text{C}$  NMR (150 MHz,  $(\text{CD}_3)_2\text{SO}$ ):  $\delta$  (ppm) = 166.7, 155.8, 155.7, 150.5, 150.0, 149.6, 149.4, 142.7, 139.9, 139.1, 139.0, 129.4, 129.3, 127.4, 127.3, 127.2, 127.1, 118.3, 117.7, 117.6, 115.5, 66.0, 37.5, 24.6, 22.4. MS (MALDI-TOF)  $m/z$  1057.57. Calcd: 1057.36. Anal. Calcd for  $\text{C}_{69}\text{H}_{76}\text{N}_4\text{O}_6$ : C, 78.38; H, 7.24, N, 5.30. Found: C, 78.07; H, 7.56, N, 5.21.

#### 2.5.9. 2,3-bis((E)-2-(10-(4-methoxyphenyl)-10H-phenothiazin-3-yl)vinyl)quinoxaline-6-carboxylic acid (**NQX3**)

**NQX3** was synthesized with a method similar to **NQX1**. A mixture of **7** (0.75 g, 3.71 mmol), **5a** (2.72 g, 8.16 mmol) and a small portion of piperidine in anhydrous toluene (20 ml) was refluxed under a  $\text{N}_2$  condition. The reaction was confirmed using thin layer chromatography. After cooling to room temperature, the remaining liquid was concentrated and purified by column chromatography on silica gel using chloroform/methanol (20:1) as an eluent to produce a red-brown solid product (1.0 g, 32%). m.p. 230 °C.  $^1\text{H}$  NMR (300 MHz,  $(\text{CD}_3)_2\text{SO}$ ):  $\delta$  (ppm) = 13.30 (br, 1H, -COOH), 8.46 (s, 1H, ArH), 8.14–8.11 (d,  $J$  = 8.7 Hz, 1H, ArH), 8.01–7.98 (d,  $J$  = 8.7 Hz, 1H, ArH), 7.86–7.84 (m, 4H, ArH,  $-\text{CH}-$ ), 7.75–7.73 (s, 2H, ArH), 7.41–7.36 (m, 6H, ArH,  $-\text{CH}-$ ), 7.25–7.22 (d,  $J$  = 9.0 Hz, 4H, ArH), 7.11–7.08 (d,  $J$  = 7.2 Hz, 2H, ArH), 6.97–6.84 (m, 4H, ArH), 6.14–6.10 (d,  $J$  = 8.4 Hz, 4H, ArH), 3.88 (s, 6H,  $-\text{CH}_3$ ).  $^{13}\text{C}$  NMR (150 MHz,  $(\text{CD}_3)_2\text{SO}$ ):  $\delta$  (ppm) = 166.7, 159.1, 150.2, 149.7, 144.6, 144.5, 143.1, 142.7, 140.0, 137.1, 136.6, 132.1, 131.8, 130.5, 130.4, 130.3, 128.6, 128.5, 128.4, 127.3, 126.6, 125.3, 122.8, 119.8, 119.0, 118.2, 116.3, 115.7, 115.3, 55.4. MS (MALDI-TOF)  $m/z$  831.64. Calcd: 832.99. Anal. Calcd for  $\text{C}_{51}\text{H}_{36}\text{N}_4\text{O}_4\text{S}_2$ : C, 73.54; H, 4.36, N, 6.73; S, 7.70. Found: C, 73.26; H, 4.68, N, 6.47; S, 7.48.



**Scheme 1.** Synthesis of **NQX1-4**. (a) aniline,  $K_2CO_3$ , Cu, CuI, *o*-dichlorobenzene, reflux, 24 h; (b)  $POCl_3$ , DMF,  $0\text{ }^\circ\text{C}$ – $80\text{ }^\circ\text{C}$ , 12 h; (c) phenothiazine,  $K_2CO_3$ , Cu, CuI, *o*-dichlorobenzene, reflux, 24 h; (d)  $POCl_3$ , DMF,  $0\text{ }^\circ\text{C}$ – $80\text{ }^\circ\text{C}$ , 12 h; (e)  $SnCl_2$ , EtOH, reflux, 5 h, 2,3-butandione, reflux, 1 h; (f) **3** or **5**, piperidine, toluene, reflux.

### 2.5.10. 2,3-bis(*E*)-2-(10-(4-methoxyphenyl)-10*H*-phenothiazin-3-yl)vinylquinoxaline-6-carboxylic acid (**NQX4**)

**NQX4** was synthesized with a method similar to **NQX1**. A mixture of **7** (0.75 g, 3.71 mmol), **5b** (3.19 g, 8.16 mmol) and a small portion of piperidine in anhydrous toluene (20 ml) was refluxed under a  $N_2$  condition. The reaction was confirmed using thin layer chromatography. After cooling to room temperature, the remaining liquid was concentrated and purified by column chromatography on silica gel using chloroform/methanol (20:1) as an eluent to produce a red-brown solid product (0.9 g, 26%), m.p.  $275\text{ }^\circ\text{C}$ .  $^1H$  NMR (300 MHz,  $(CD_3)_2SO$ ):  $\delta$  (ppm) = 13.42 (br, 1H, -COOH), 8.46 (s, 1H, ArH), 8.16–8.13 (d,  $J = 8.7$  Hz, 1H, ArH), 7.99–7.96 (d,  $J = 8.7$  Hz, 1H, ArH), 7.86–7.84 (m, 4H, ArH, -CH-), 7.75–7.72 (m, 2H, ArH), 7.38–7.35 (m, 6H, ArH, -CH-), 7.24–7.21 (d,  $J = 9.0$  Hz, 4H, ArH), 7.11–7.08 (d,  $J = 7.2$  Hz, 2H, ArH), 6.96–6.84 (m, 4H, ArH), 6.15–6.12 (d,  $J = 8.7$  Hz, 4H, ArH), 4.13–4.09 (t,  $J = 6.6$  Hz, 4H, -CH<sub>2</sub>-), 1.89–1.80 (m,  $J = 6.6$  Hz, 2H, -CH-), 1.72–1.65 (q,  $J = 6.6$  Hz, 4H, -CH<sub>2</sub>-), 0.99–0.97 (d, 12H, -CH<sub>3</sub>).  $^{13}C$  NMR (150 MHz,  $(CD_3)_2SO$ ):  $\delta$  (ppm) = 166.7, 158.5, 150.2, 149.7, 144.6, 144.5, 143.2, 143.1, 142.7, 140.0, 137.5, 137.1, 131.9, 131.7, 130.5, 130.4, 130.2, 128.6, 128.4, 128.3, 127.3, 126.5, 125.4, 122.8, 119.0, 118.2, 116.7, 115.7, 115.4, 66.3, 37.5, 24.6, 22.5. MS (MALDI-TOF)  $m/z$  944.55, Calcd: 945.20. Anal. Calcd for  $C_{59}H_{52}N_4O_4S_2$ : C, 74.97; H, 5.55, N, 5.93; S, 6.78. Found: C, 74.75; H, 5.83, N, 5.65; S, 6.47.

## 3. Result and discussion

### 3.1. Synthesis

The synthetic routes followed to prepare compounds are presented in **Scheme 1**. The triphenylamine and phenothiazine aldehydes were prepared according to reported procedures and the analytical data are presented in the supporting information. The starting compound **2**, 3-dimethylquinoxaline-6-carboxylic acid, **7** was prepared by the reported method [30]. The  $^1H$  NMR spectra showed that the methyl proton of compound **7** were observed at 2.71 ppm. Due to the strong electron withdrawing effect of the carboxy group and the quinoxaline ring, the methyl group of **7** was able to undergo a condensation reaction with arylaldehydes.

Starting from the corresponding aldehyde derivatives **3** or **5** and **7** in the presence of piperidine and toluene as solvent, the target compounds were prepared through a Knoevenagel condensation. On the other hand, the  $^1H$  NMR spectrum of **NQX1-4** indicated that the ethylene protons appeared as doublets at 7.90–7.95 ppm ( $J = 15.3$  Hz), and 7.67–7.72 ppm ( $J = 15.3$  Hz). According to the coupling constant, **NQX1-4** should exist in the *trans*-configuration (**Fig. 1**).

### 3.2. UV–vis absorption property

The results of computational calculations (**Fig. 3**) revealed that the basic chromophores of the target compounds have strong intramolecular charge transfer (ICT) system in which the alkoxyaminophenyl unit acts as a donor and the quinoxaline unit as an acceptor moiety. **Fig. 2** shows the UV–vis spectra of **NQX1-4** in chloroform solution. The synthesized sensitizers showed a broad absorption band up to approximately 600 nm. **NQX1** and **NQX2** have three absorption peaks. The two peaks located near 300 and 400 nm resulted from two triphenylamine groups as light absorbing antennae and an efficient  $\pi$ - $\pi^*$  transition [31]. The peak near 500 nm caused intramolecular charge transfer (ICT) between

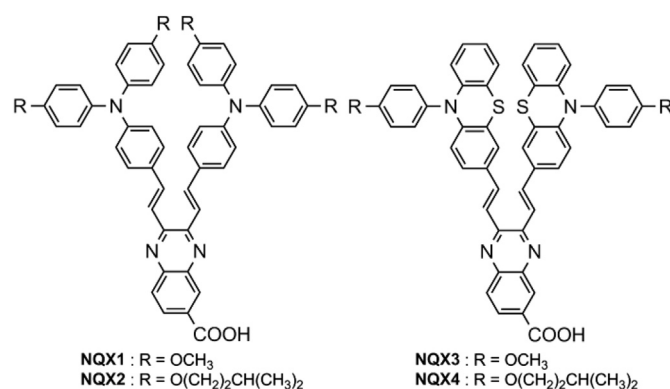


**Fig. 1.** Molecular structures of quinoxaline-based dyes.

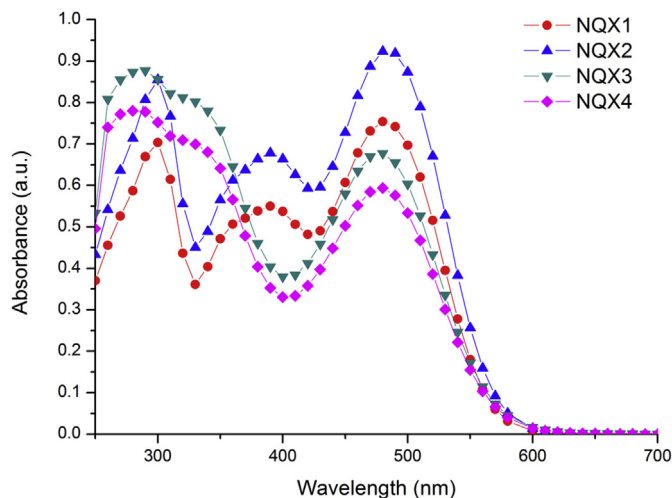


Fig. 2. Absorption spectra of dyes in a chloroform solution ( $2.0 \times 10^{-5}$  M).

the donor and acceptor. Similarly, **NQX3** and **NQX4** showed strong absorption peaks near 350 and 500 nm. The  $\lambda_{\max}$  values of **NQX1** and **NQX2** substituted with tetra-alkoxy groups on the triphenylamine exhibited a slight red-shift absorption compared to those of

**NQX3** and **NQX4**. Their molar coefficient ( $\epsilon$ ) were observed in the range of  $29,700$ – $46,300$   $\text{M}^{-1} \text{cm}^{-1}$ .

### 3.3. Electrochemical property

Cyclovoltametry was used to measure the electrochemical property of the synthesized sensitizers in DMF with a three electrode configuration consisting of a carbon disk working electrode, a Ag/AgCl reference electrode and a Pt wire counter electrode. 0.1 M tetra-*n*-butylammonium tetrafluoroborate (TBABF<sub>4</sub>) in a DMF solution was used as the supporting electrolyte. The highest occupied molecular orbital (HOMO) level was calculated using HOMO (eV) =  $-4.8 - (E_{\text{onset}} - E_{1/2}(\text{Ferrocene}))$ . The  $E_{\text{onset}}$  is the oxidation potential (V) and  $E_{1/2}(\text{Ferrocene})$  is the half-wave potential in solution. The band gap ( $E_g$ ) was derived from the wavelength at a 10% maximum absorption intensity. The lowest unoccupied molecular orbital (LUMO) level was estimated using LUMO = HOMO +  $E_g$ .

The electrochemical properties of the dyes are shown in Table 1. The dyes showed similar energy levels. The HOMO levels of the dyes were less than the redox level of  $\text{I}^-/\text{I}^{3-}$  ( $-4.6$  eV), indicating that the HOMO levels were adequate for efficient dye regeneration. The LUMO levels were greater than the conduction band of the metal oxide semiconductor ( $-3.8$  eV, TiO<sub>2</sub>), implying that excited electrons can be efficiently injected into the semiconductor. Therefore, the electrochemical properties of the dyes were appropriate for DSSC.

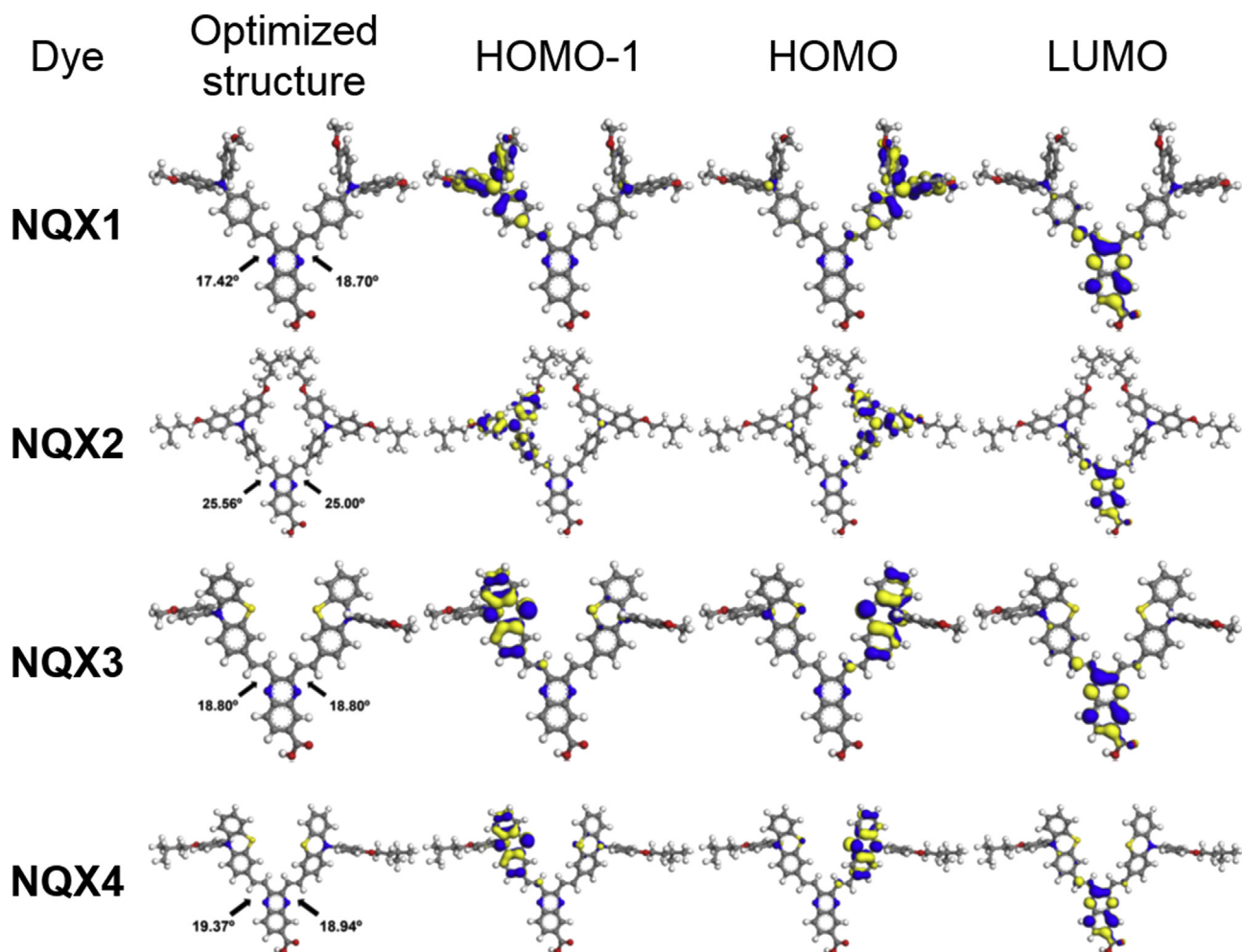


Fig. 3. Optimized structures and electronic distributions in the HOMO, HOMO-1 and LUMO levels of the dyes.

**Table 1**  
Photophysical and electrochemical properties of **NQX1-4**.

Dyes	$\lambda_{\max}^a$ (nm)	$\epsilon^a$ ( $M^{-1}cm^{-1}$ )	$F_{\max}^b$ (nm)	HOMO <sup>c</sup>	$E_g^d$	LUMO <sup>e</sup>
<b>NQX1</b>	482	37,700	684	−4.98	2.20	−2.78
<b>NQX2</b>	484	46,300	685	−4.99	2.19	−2.80
<b>NQX3</b>	477	33,900	698	−4.92	2.18	−2.75
<b>NQX4</b>	478	29,700	699	−4.92	2.17	−2.75

<sup>a</sup> Measured in a chloroform solution ( $2.0 \times 10^{-5}$  M).

<sup>b</sup> Excited at their  $\lambda_{\max}$  values.

<sup>c</sup> HOMO =  $-4.8 - (E_{\text{onset}} - E_{1/2}(\text{Ferrocene}))$ ,  $E_{\text{onset}}$  was determined from the oxidation onset, scan rate: 100  $mVs^{-1}$ .

<sup>d</sup> Measured from the 10% intensity of  $\lambda_{\max}$ .

<sup>e</sup> LUMO = HOMO +  $E_g$ .

### 3.4. Theoretical approach

Geometric optimization of the designed structure using computational calculations was applied to explain the minimal effect of the substituent. Accelrys Materials Studio 4.3 was used for molecular design and the calculation employed the Forcite tool (molecular mechanics) and VAMP (semi-empirical method) with PM3 Hamiltonian methods.

Fig. 3 shows the electron distribution of the HOMO and LUMO of dyes and the dihedral angles between the quinoxaline ring and adjacent ethylene moieties. The HOMO-1 and HOMO levels represent the highest electron density near triphenylamine or phenothiazine moieties as the electron donor, while LUMO is located near the quinoxaline unit as the electron acceptor suggesting that the photo-induced electron transfer occurs more efficiently.

The donor groups of the optimized structures are located as far from each other as possible to avoid overlap. The dihedral angles of **NQX1** ( $17.42^\circ$  and  $18.70^\circ$ ) between the electron donor and quinoxaline ring are larger than those of **NQX2** ( $25.56^\circ$  and  $25.00^\circ$ ) due to steric strain, which results from the increased presence of bulkier isopentyloxy moieties over methoxy moieties. The optimized structures of **NQX3-4** show that only alkoxy phenyl rings are distorted significantly, with the exception of other rings linked by sulfur atoms. The dihedral angles for **NQX3** are slightly smaller than those for **NQX4** due to the varied bulkiness of the alkoxy moieties.

### 3.5. Solar cell performance

The effects of the electron donors with an alkoxy chain on the efficiency of the cells were evaluated by measuring their cell performance relative to **N719** as the reference dye. The photocurrent density-voltage ( $J$ - $V$ ) curves and the IPCE spectra of DSSCs based on the synthesized dyes are shown in Fig. 4, and the numerical results are summarized in Table 2. A photomask was used to prevent the

**Table 2**  
Photovoltaic performance of the dyes.

Dye	$V_{oc}$ (V)	$J_{sc}$ ( $mA/cm^2$ )	FF	$\eta$ (%)
<b>N719</b>	0.69	12.77	0.75	6.57
<b>NQX1</b>	0.65	8.72	0.73	4.10
<b>NQX2</b>	0.70	7.60	0.75	3.98
<b>NQX3</b>	0.64	9.77	0.67	4.18
<b>NQX4</b>	0.61	9.99	0.71	4.36

over-measured photocurrent due to light scattering near the edge of the active area [32].

Under AM 1.5 illumination, the **NQX4**-based cells showed the best photovoltaic performance among **NQX1-4**. The cell with **NQX4** exhibited a short circuit current density ( $J_{sc}$ ) of  $9.99 mA/cm^2$ , an open circuit voltage ( $V_{oc}$ ) of 0.61 V, and a fill factor (FF) of 0.71, resulting in an overall power conversion efficiency  $\eta$  of 4.36%.

The cell fabricated with **NQX1** has higher efficiency than that with **NQX2**, possibly caused by a large difference in distortions between triphenylamine and quinoxaline groups leading to a lower  $J_{sc}$  [27]. The efficiency of **NQX4** is slightly higher than that of **NQX3**. It might be ascribed to rise in photo-to-current conversion efficiency is influenced by the varied electron donating ability of alkoxy chains.

According to the IPCE spectra, the synthesized dye based cells had high maximum IPCE values near the wavelength of 500 nm, which were greater than 70%. The **NQX4**-based cell had an IPCE value of 81% at 490 nm, which was much greater than the maximum IPCE value of the **N719**-based cell. The fabricated cells had onsets of their IPCE spectra below 700 nm. Though the cell fabricated with **NQX4** had a lower overall efficiency than **N719** due to narrow light absorption, further modifications of the structure would lead to red-shift of the absorption band and improvements in the conversion efficiency of the cell.

## 4. Conclusion

We successfully designed and synthesized quinoxaline-based dyes (**NQX1-4**) containing triphenylamine and phenothiazine derivatives with alkoxy moieties as an electron donor. The triphenylamine and phenothiazine derivatives with alkoxy chains and the quinoxaline group were shown as an efficient electron donor and acceptor for DSSC, respectively. The cells fabricated with **NQX3** and **NQX4** using phenothiazine moieties had greater overall efficiency than the cells fabricated with **NQX1** and **NQX2** using triphenylamine moieties. The solar cell based on **NQX4** showed the best power conversion efficiency of 4.36% and a high IPCE value near 500 nm. These results indicate that further study of metal-free

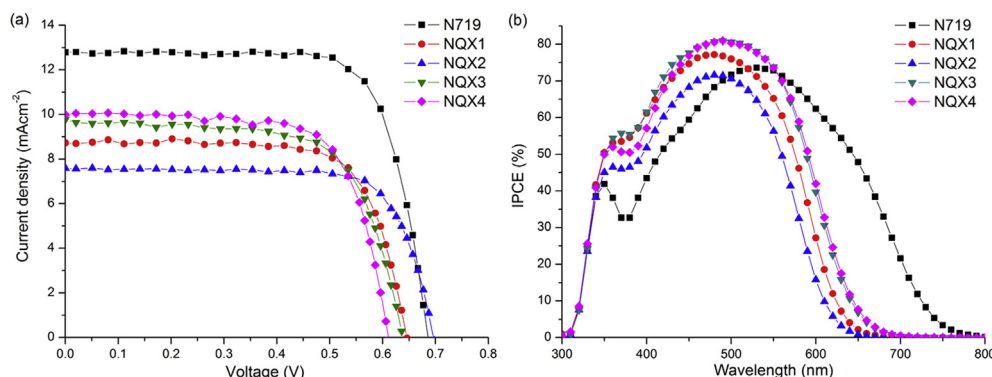


Fig. 4. (a)  $J$ - $V$  curves and (b) IPCE spectra of the DSSCs based on **N719**, **NQX1**, **NQX2**, **NQX3**, and **NQX4**.

organic dyes may lead to the development of a high-efficiency solar cell.

## Acknowledgment

This work was supported by the Technology Innovation Program (No. 10047756, Development of tetra-pyrrole type for Color, light-emitting, detecting Devices) funded by the Ministry of Trade, Industry & Energy (MI, Korea).

## Appendix A. Supplementary data

Supplementary data related to this article can be found at <http://dx.doi.org/10.1016/j.dyepig.2015.05.019>.

## References

- [1] O'Regan B, Grätzel M. A low-cost, high-efficiency solar cell based on dye-sensitized colloidal TiO<sub>2</sub> films. *Nature* 1991;353:737–40.
- [2] Hagfeldt A, Boschloo G, Sun L, Kloo L, Pettersson H. Dye-sensitized solar cells. *Chem Rev* 2010;110(10):6595–663.
- [3] Clifford JN, Martinez-Ferrero E, Viterisi A, Palomares E. Sensitizer molecular structure–device efficiency relationship in dye sensitized solar cells. *Chem Soc Rev* 2011;40(3):1635–46.
- [4] Gao F, Wang Y, Shi D, Zhang J, Wang M, Jing X, et al. Enhance the optical absorptivity of nanocrystalline TiO<sub>2</sub> film with high molar extinction coefficient ruthenium sensitizers for high performance dye-sensitized solar cells. *J Am Chem Soc* 2008;130(32):10720–8.
- [5] Kakiage K, Aoyama Y, Yano T, Oya K, Kyomen T, Hanaya M. Fabrication of a high-performance dye-sensitized solar cell with 12.8% conversion efficiency using organic silyl-anchor dyes. *Chem Commun* 2015;51(29):6315–7.
- [6] Wang Z-S, Cui Y, Dan-oh Y, Kasada C, Shinpo A, Hara K. Thiophene-functionalized coumarin dye for efficient dye-sensitized solar cells : electron lifetime improved by coadsorption of deoxycholic acid. *J Phys Chem C* 2007;111(19):7224–30.
- [7] Ito S, Miura H, Uchida S, Takata M, Sumioka K, Liska P, et al. High-conversion-efficiency organic dye-sensitized solar cells with a novel indoline dye. *Chem Commun* 2008;(41):5194–6.
- [8] Matsui M, Tanaka N, Ono Y, Kubota Y, Funabiki K, Jin J, et al. Performance of new single rhodanine indoline dyes in zinc oxide dye-sensitized solar cell. *Sol Energy Mater Sol Cells* 2014;128:313–9.
- [9] Ripolles-Sanchis T, Guo BC, Wu HP, Pan TY, Lee HW, Raga SR, et al. Design and characterization of alkoxy-wrapped push-pull porphyrins for dye-sensitized solar cells. *Chem Commun* 2012;48(36):4368–70.
- [10] Yella A, Lee H-W, Tsao HN, Yi C, Chandiran AK, Nazeeruddin MK, et al. Porphyrin-sensitized solar cells with cobalt (II/III)-Based redox electrolyte exceed 12 percent efficiency. *Science* 2011;334:629–34.
- [11] Li C, Yum JH, Moon SJ, Herrmann A, Eickemeyer F, Pschirer NG, et al. An improved perylene sensitizer for solar cell applications. *ChemSusChem* 2008;1(7):615–8.
- [12] Yan C, Ma W, Ren Y, Zhang M, Wang P. Efficient triarylamine–perylene dye-sensitized solar cells: influence of triple-bond insertion on charge recombination. *ACS Appl Mater Interfaces* 2015;7(1):801–9.
- [13] Mori S, Nagata M, Nakahata Y, Yasuta K, Goto R, Kimura M, et al. Enhancement of incident photon-to-current conversion efficiency for phthalocyanine-sensitized solar cells by 3D molecular structuralization. *J Am Chem Soc* 2010;132:4054–5.
- [14] Ragoussi ME, Yum JH, Chandiran AK, Ince M, de la Torre G, Grätzel M, et al. Sterically hindered phthalocyanines for dye-sensitized solar cells: influence of the distance between the aromatic core and the anchoring group. *Chemphyschem* : a Eur J Chem Phys Phys Chem 2014;15(6):1033–6.
- [15] Tian H, Yang X, Chen R, Pan Y, Li L, Hagfeldt A, et al. Phenothiazine derivatives for efficient organic dye-sensitized solar cells. *Chem Commun* 2007;(36):3741–3.
- [16] Tian H, Yang X, Cong J, Chen R, Teng C, Liu J, et al. Effect of different electron donating groups on the performance of dye-sensitized solar cells. *Dyes Pigments* 2010;84(1):62–8.
- [17] Bae SH, Seo KD, Kim HK. A near-IR organic sensitizer with squaraine and phenothiazine unit for dye-sensitized solar cells. *Mol Cryst Liq Cryst* 2014;600(1):116–22.
- [18] Hung WI, Liao YY, Hsu CY, Chou HH, Lee TH, Kao WS, et al. High-performance dye-sensitized solar cells based on phenothiazine dyes containing double anchors and thiophene spacers. *Chem Asian J* 2014;9(1):357–66.
- [19] Yun HJ, Jung DY, Lee DK, Jen AKY, Kim JH. Panchromatic quasi-solid-state squaraine dye sensitized solar cells enhanced by Förster resonance energy transfer of DCM–pyran. *Dyes Pigments* 2015;113:675–81.
- [20] Mathew S, Yella A, Gao P, Humphry-Baker R, Curchod BF, Ashari-Astani N, et al. Dye-sensitized solar cells with 13% efficiency achieved through the molecular engineering of porphyrin sensitizers. *Nat Chem* 2014;6(3):242–7.
- [21] Ning Z, Tian H. Triarylamine: a promising core unit for efficient photovoltaic materials. *Chem Commun* 2009;(37):5483–95.
- [22] Hagberg DP, Yum J-H, Lee H, Angelis FD, Marinado T, Karlsson KM, et al. Molecular engineering of organic sensitizers for dye-sensitized solar cell applications. *J Am Chem Soc* 2008;(130):6259–66.
- [23] Kim SH, Sakong C, Chang JB, Kim B, Ko MJ, Kim DH, et al. The effect of N-substitution and ethylthio substitution on the performance of phenothiazine donors in dye-sensitized solar cells. *Dyes Pigments* 2013;97(1):262–71.
- [24] Pei K, Wu Y, Islam A, Zhu S, Han L, Geng Z, et al. Dye-sensitized solar cells based on quinoxaline dyes: effect of  $\pi$ -linker on absorption, energy levels, and photovoltaic performances. *J Phys Chem C* 2014;118(30):16552–61.
- [25] Chang DW, Lee HJ, Kim JH, Park SY, Park S-M, Dai L, et al. Novel quinoxaline-based organic sensitizers for dye-sensitized solar cells. *Org Lett* 2011;13(15):3880–3.
- [26] Kono T, Murakami TN, Nishida J-i, Yoshida Y, Hara K, Yamashita Y. Synthesis and photo-electrochemical properties of novel thienopyrazine and quinoxaline derivatives, and their dye-sensitized solar cell performance. *Org Electron* 2012;13(12):3097–101.
- [27] Shi J, Chai Z, Su J, Chen J, Tang R, Fan K, et al. New sensitizers bearing quinoxaline moieties as an auxiliary acceptor for dye-sensitized solar cells. *Dyes Pigments* 2013;98(3):405–13.
- [28] Said SA, Fiksdahl A, Carlsen PHJ. Stereoselective synthesis of optically active phenyl ethers. *Tetrahedron Lett* 2000;41:5593–6.
- [29] Mimaite V, Ostrauskaite J, Gudeika D, Grazulevicius JV, Jankauskas V. Structure–properties relationship of hydrazones containing methoxy-substituted triphenylamino groups. *Synth Met* 2011;161(15–16):1575–81.
- [30] Qiu J, Xu B, Huang Z, Pan W, Cao P, Liu C, et al. Synthesis and biological evaluation of Matijing-Su derivatives as potent anti-HBV agents. *Bioorg Med Chem* 2011;19(18):5352–60.
- [31] Chen H, Huang H, Huang X, Clifford JN, Forneli A, Palomares E, et al. High molar extinction coefficient branchlike organic dyes containing di(p-tolyl) phenylamine donor for dye-sensitized solar cells applications. *J Phys Chem C* 2010;114(7):3280–6.
- [32] Ito S, Nazeeruddin MK, Liska P, Comte P, Charvet R, Péchy P, et al. Photovoltaic characterization of dye-sensitized solar cells: effect of device masking on conversion efficiency. *Prog Photovoltaics: Res Appl* 2006;14(7):589–601.